Journal of Polymer Research (2024) 31:288
https://doi.org/10.1007/s10965-024-04120-2

ORIGINAL PAPER

Preparation of slippery liquid-infused porous surface with high stability by SiO_2-assisted polyimide porous membrane

Yawen Guo[1] · Li Yang[1] · Chengcheng Lv[1] · Chongyang Mai[1] · Lielun Zhao[1] · Yan Jiang[1] · Hongwen Zhang[1]

Received: 23 February 2023 / Accepted: 12 August 2024

Abstract
Inspired by nepenthes pitcher plants, the slippery liquid-infused porous surfaces have received extensive attention. In its practical application, good oil storage and oil-locking ability are important guarantee for the surface to maintain the interface performance for a long time. In this paper, mesoporous silica (KCC-1) was obtained by cetyltrimethylammonium bromide (CTAB) as template agent, urea as a hydrolyzing agent, and TEOS as silicon source reagent, then modified with (3-Aminopropyl) trimethoxysilane. Then combined with the breath figures, amino-modified mesoporous silica, 3,3'-4,4'-biphenyltetracarboxylic dianhydride (S-BPDA), 2,2'-bis[4-(4-aminophenoxyphenyl)]propane (BAPP) were used as raw materials to prepare polyimide SLIPS with good stability by a two-step method. The wettability and stability of SLIPS were investigated, and the results show that the introduction of mesoporous silica inorganic nanoparticles enhanced the performance of SLIPS. Among them, the sliding angle of polyimide SLIPS with a nanoparticle content of 10% is 2°, which has good self-cleaning performance, antifouling performance, and stability.

Keywords The breath figures (BF) · Polyimide · Slippery liquid-infused porous surface · Mesoporous silica · Antifouling

Introduction

Polyimide is widely used in aerospace and electronics industries due to its excellent mechanical properties, thermal stability, and chemical resistance [1–4], polyamide acid solution which is the precursor of polyimide has excellent adhesion to glass, single crystal and metal surfaces after proper heat treatment [5]. In the past ten years, more and more researchers have begun to use polyimide to prepare porous membranes [6]. Martínez-Gómez [7] prepared an aromatic polyimide porous membrane containing PEO branches, which has high resistance to Staphylococcus aureus, and the increase of PEO content in the copolymer reduces bacterial adhesion. Breuning [8] used solvents with different boiling points and different polarities in the preparation process to generate layered pores in sponge-like polyimide, which has higher CO_2 selectivity and absorption rate. Ye [9] prepared oil-impregnated porous polyimide materials by laser scanning method and found that reasonable control of the surface pore size can improve the oil-locking rate and reduce the friction coefficient of oil-impregnated PPI materials. This provides ideas and data support for the design of SLIPS for polyimide polymers.

Micro- and nano-scale porous materials can be used in optics, biomedicine, self-cleaning and other fields [10–12]. However, in the process of its application, the micro-sized pollutants will be deposited in the micro-nano structure gap, resulting in the loss of self-cleaning performance on the surface of the porous material. To solve this problem, scientists were inspired by nepenthes pitcher plants and successfully prepared a liquid-infused porous surface with a lubricating effect, namely "slippery liquid-infused porous surface" (SLIPS) [13]. SLIPS has excellent properties such as self-cleaning [14, 15], self-healing [16], anti-icing [17, 18], and anti-fouling [19, 20]. But for SLIPS materials, the weak interaction between matrix and lubricant is its inherent disadvantage, which can lead to the loss of surface lubricant, and limit the practical application of SLIPS [21]. In practical applications, stability is an extremely important factor, and it is of great significance to prepare SLIPS with good stability.

In this paper, mesoporous silica was introduced to prepare polyimide SLIPS with good stability by the breath figures. Mesoporous silica (KCC-1) is obtained by the reaction of

✉ Hongwen Zhang
hwzhang@cczu.edu.cn

[1] School of Materials Science and Engineering, Changzhou University, Changzhou, Jiangsu, China

Published online: 17 September 2024

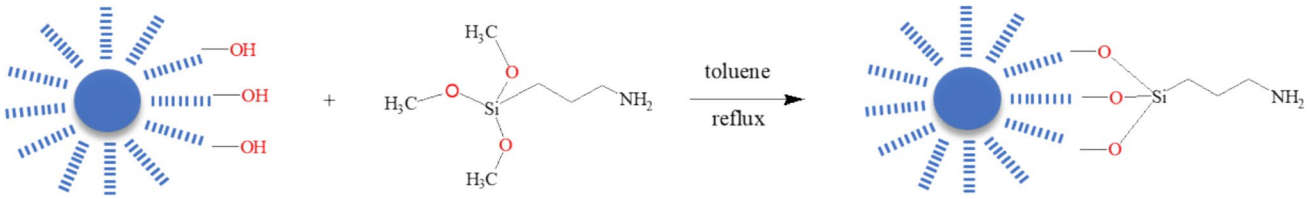

Scheme 1 The synthetic route to prepare the KCC-1-NH_2

cetyltrimethylammonium bromide (CTAB), urea, and TEOS. KCC-1 was modified with KH-540 and reacted with APT-PDMS, BAPP and S-BPDA to form polyamide acid, combined with the breath figures(BF) to prepare porous structure substrates, poured into silicone oil, and finally obtained a series of polyimide SLIPS. At present, there are few reports on the preparation of SLIPS related to polyimide. In this paper, nano-mesoporous silica was innovatively introduced into the main chain of polyimide to prepare SLIPS with excellent comprehensive performance, and their stability and sliding performance are better than those of SLIPS prepared by blending polyamide acid and mesoporous silica. This paper provides a new method for preparing durable SLIPS.

Experimental section

Materials

Octamethylcyclotetrasiloxane (D_4, 98% purity), 1,3-bis(3-aminopropyl) tetramethyldisiloxane, 3,3'-4 ,4'-biphenyltetracarboxylic dianhydride (S-BPDA) were purchased from Aladdin Reagent Co., Ltd. Tetramethylammonium hydroxide ($(Me)_4NOH$), KH540, 2,2'-bis[4-(4-aminophenoxy) phenyl]propane (BAPP) were purchased from Shanghai McLean Biochemical Technology Co., Ltd. Cetyltrimethylammonium bromide (CTAB), ethyl orthosilicate (TEOS), urea, cyclohexane, 1-pentanol, Trichloromethane (analytical grade), toluene (analytical grade) were purchased from Sinopharm Group Chemical Reagent Co., Ltd., anhydrous ethanol and N-N dimethylacetamide were purchased from Shanghai Lingfeng Chemical Reagent Co., Ltd.

Experimental process

Synthesis of KCC-1 and KCC-1-NH2

1 g of CTAB was added to10 mL distilled water and after addition of 0.5 g urea, the mixture was stirred for about 3 h at room temperature. Then, the mixture of 2 g TEOS, 30 mL cyclohexane and 1.5 mL pentanol was added to the flask and sonicated for 30 min. Afterwards, the mixture was heated at 80 °C for 4 h and subsequently refluxed at 60 °C for 24 h. The collected KCC-1 was washed with water and ethanol three times. Finally, the KCC-1 was dried in an oven at 60 °C for 24 h (Sch 1) .

Mix 5.37 g KH540, 19.3 g ethanol and 1.43 g water for 30 min sonication. At the same time, 0.6 g of KCC-1 was dispersed on 10 mL toluene and sonicated for 30 min. Then KH540, ethanol and water were poured into toluene, refluxed at 80 °C for 24 h, the precipitate was washed three times with ethanol and dried at 80 °C for 24 h to obtain KCC-1-NH_2.

Synthesis of APT-PDMS

The mixture of 29.7 g octamethylcyclotetrasiloxane (D_4), 2.5 g 1,3-bis(3-aminopropyl) tetramethyldisiloxane and 0.6 g $(Me)_4NOH$ was added to the three-necked flask reacted at 105 °C in a dry nitrogen environment. After 18 h of reaction, the system was heated to 180 °C to degrade the catalyst, and the temperature was lowered to below 160 °C to remove low-boiling small molecular impurities and other by-products. Finally a colorless viscous amino-terminated polydimethylsiloxane (APT-PDMS) liquid is obtained.

Synthesis of polyamide acid

Weigh an appropriate amount of KCC-1-NH_2, APT-PDMS, BAPP and dissolve them in DMAc solution (12 wt%) and stir for 30 min. Then S-BPDA was added three times. The system was reacted in a vacuum state at room temperature for three hours to obtain a polyamide acid, and the obtained polyamide acid was dried in a vacuum oven at 100 °C. Without introducing APT-PDMS, KCC-1-NH_2 and APT-PDMS, two groups of control polyamide acids were prepared in the same way, named P1 and P2 respectively (Table 1).

Weigh an appropriate amount of P2 and KCC-1 for blending to prepare SLIPS (the content is shown in Table 2), and name them as 1, 2, 3 and 4 respectively.

Preparation of SLIPS

Porous honeycomb films were prepared by using the BF method. First, copolymer (30 mg) was dissolved in $CHCl_3$

Table 1 Monomer addition formula of PI copolymer

Samples	KCC-1-NH_2	APT-PDMS	BAPP	S-BPDA	KCC-1-NH_2 ratio	SiO_2:APT-PDMS
P1	0	0	0.8210 g	0.5938 g		
P2	0	2.1024 g	0.5747 g	0.5938 g		
P3	0.1447 g	1.7557 g	0.4310 g	0.5938 g	5%	1:12
P4	0.2894 g	1.5768 g	0.4310 g	0.5938 g	10%	1:2.5
P5	0.7236 g	1.1461 g	0.4310 g	0.5938 g	25%	1.5:1
P6	1.1570 g	0.7112 g	0.4310 g	0.5938 g	40%	1.6:1

Table 2 Monomer dosage formula prepared by blending PI and KCC-1

Samples	P2	KCC-1	KCC-1 ratio
1	28.5 g	1.5 g	5%
2	27 g	3 g	10%
3	22.5 g	7.5 g	25%
4	18 g	12 g	40%

(1 mL) solvent, and sonicate the solution for 10 min to ensure complete dissolution. Take 100 ~ 200 µL casting solution to the 2 × 2 cm^2 glass piece by pipette and allowed to self-assemble in a constant temperature water tank at 40 °C for one hour. The obtained porous substrates were cured at high temperatures: 100, 200, and 300 °C solidify 1 h, respectively. Finally, polydimethylsiloxane was poured, and the glass slide was placed vertically for at least 12 h to obtain a series of PI SLIPS (Sch 2) .

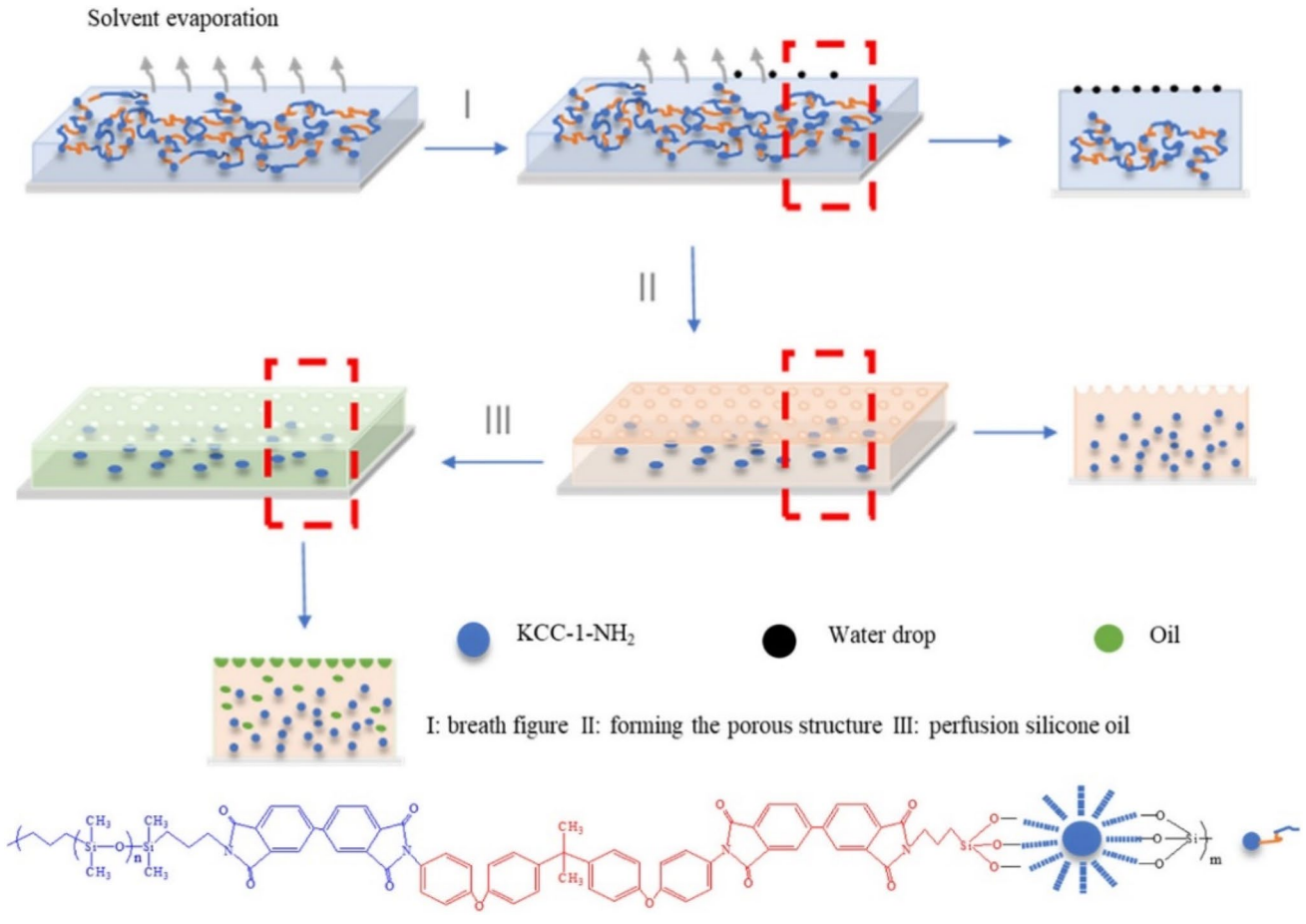

Scheme 2 Shceme2 Preparation process of SLIPS

Characterizations

The structures and compositions of the PI materials were characterized by Nicolet Avatar 370 Fourier transform infrared spectrometer (Wisconsin, America), APT-PDMS, KCC-1 and KCC-1-NH_2 use KBr tableting for sample preparation, with 16 scanning times; polyimide uses ATR, with 32 scanning times, and the scanning range is 400–4000 cm^{-1}. Thermogravimetric analysis (TGA) was measured on a Netzsch thermal analysis system(Selbu, Germany) at a scan rate of 20 °C/min in N_2. ZEN3600 laser particle size analyzer was used for the zeta potential test. The water contact angle was tested with a Zhongchen JC2000D1 at room temperature. Water and some common liquids are used as solvents and control the droplet size to 5 μL. The surface morphologies of the porous substrates were investigated by scanning electron microscopy (SEM) on JSM-IT100 from JEOL. The oil retention was recorded per 10 min using the YJ-250 A glue dispenser of Beijing Jie Yali Technology Co., Ltd. The operation revolving speed was 3000 rpm. The oil content and oil retention were calculated with the following equations:

$$Oil\ retention = \frac{m_i - m_0}{m - m_0} \times 100\% \quad (2)$$

In the formula, m_0 is the weight of pure porous substrate, m is the weight of porous substrate impregnated with lubricants, and m_i is the weight of porous substrate impregnated with lubricants after being centrifuged for a period of time(t).

Results and discussion

Modification analysis of KCC-1

FTIR was applied to approve the proper functionalization of the KCC-1 with -NH_2. As shown in Fig. 1(a), the characteristic peaks of the silica based materials could be observed in the range of 1013 to 1112 cm^{-1} representing the Si-O-Si asymmetric stretching and Si-OH peak is observed at 850 cm^{-1} which representsthe stretching vibration and asymmetric bending.

The zeta potential of KCC-1 and KCC-1-NH_2 dispersed in distilled water was detected. The surface of KCC-1 is rich in hydroxyl groups and displays negative charge(-13.2 mv). However, after modification, the zeta potential of KCC-1-NH_2 is 16.7 mV, which is due to the reaction between APTS and KCC-1 to form a covalent bond, showing a positive charge.

Thermogravimetric analysis of KCC-1 and KCC-1-NH_2 was carried out under a nitrogen atmosphere. The thermogram of KCC-1-NH_2 (Fig. 1b) shows that the total weight loss is approximately 21.55% of its initial weight: The first stage is below 140 ℃, and its weight loss mainly comes from the evaporation of water. In the second stage, in the range of 150–700 ℃, the weight loss rate of KCC-1-NH_2 (b) was higher than that of KCC-1 (a), mainly due to the grafted APTS molecules from the surface of KCC-1. These results again demonstrate the successful modification of KCC-1.

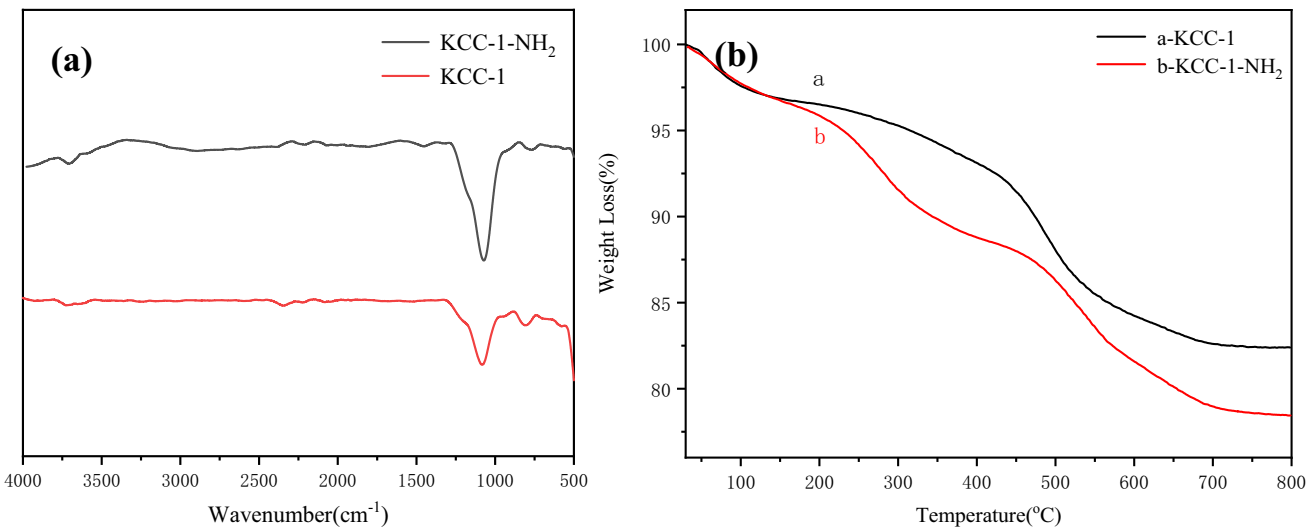

Fig. 1 (**a**) FT-IR Spectra of KCC-1 and KCC-1-NH_2 (**b**)TGA analysis of KCC-1 and KCC-1-NH_2

Structural and compositional characterization and thermal stability analysis

FTIR indicates the successful synthesis of APT-PDMS. As shown in Fig. 2(a), the stretching vibration absorption peak of -NH_2 appears at 3392 cm^{-1}, the peaks at 2905 cm^{-1} and 2962 cm^{-1} come from the stretching vibration absorption peak of the methyl group connected to silicon atoms in the main chain and the characteristic peaks of the silica based materials could be observed in the range of 1020 to 1094 cm^{-1} representing the Si-O-Si asymmetric stretching.

Curve a in Fig. 2(b) is the infrared absorption of the polyimide film without polysiloxane. The asymmetric and symmetric carboxyl strength of the imide ring around 1772, 1719 cm^{-1}, C-N stretching around 1363 cm^{-1} are characteristics of polyimide, indicating that the polyimide was successfully prepared in the experiment. Compared curve a, curve b has stretching vibration absorption peaks of -Si-O-Si- at 1010 cm^{-1} and 1069 cm^{-1}, which proved the successful introduction of APT-PDMS into the polyimide film. Curve c is the infrared spectrum of the nano-silica treated by ultrasonic and centrifugation after polymerization. The features of P4 are further demonstrated by peaks at 1771 cm^{-1} (C = O asymmetric stretching), 1718 cm^{-1} (C = O asymmetric stretching), 1380 cm^{-1} (C-N asymmetric stretching), which proved the successful introduction of KCC-1-NH_2 into the reaction chain.

The thermal stability of P1, P2 and P4 were investigated by thermogravimetric analysis, as shown in Fig. 2(c) and (d). The temperature of 10% weight loss of P1, P2 and P4 is 572 ℃, 482 ℃ and 509 ℃ respectively, all above 450 ℃. After the introduction of APT-PDMS and KCC-1-NH_2, flexible macromolecular and rigid nanoparticles became a component of polyimide composites, which destroyed the regularity and symmetry of the polyimide, resulting in the thermal decomposition temperature of P2 and P4 is lower than P1. The decomposition of P4 around 400 °C is caused by the decomposition of APTS. Overall, the three groups of PIs have good thermal stability.

SEM analysis of porous substrates

Figure 3(a) shows the scanning electron microscopy of KCC-1. It can be seen that KCC-1 is spherical as a whole, the surface is not smooth, shows a wrinkled shape, and the particle size is relatively uniform, indicating that KCC-1 microspheres were successfully prepared.

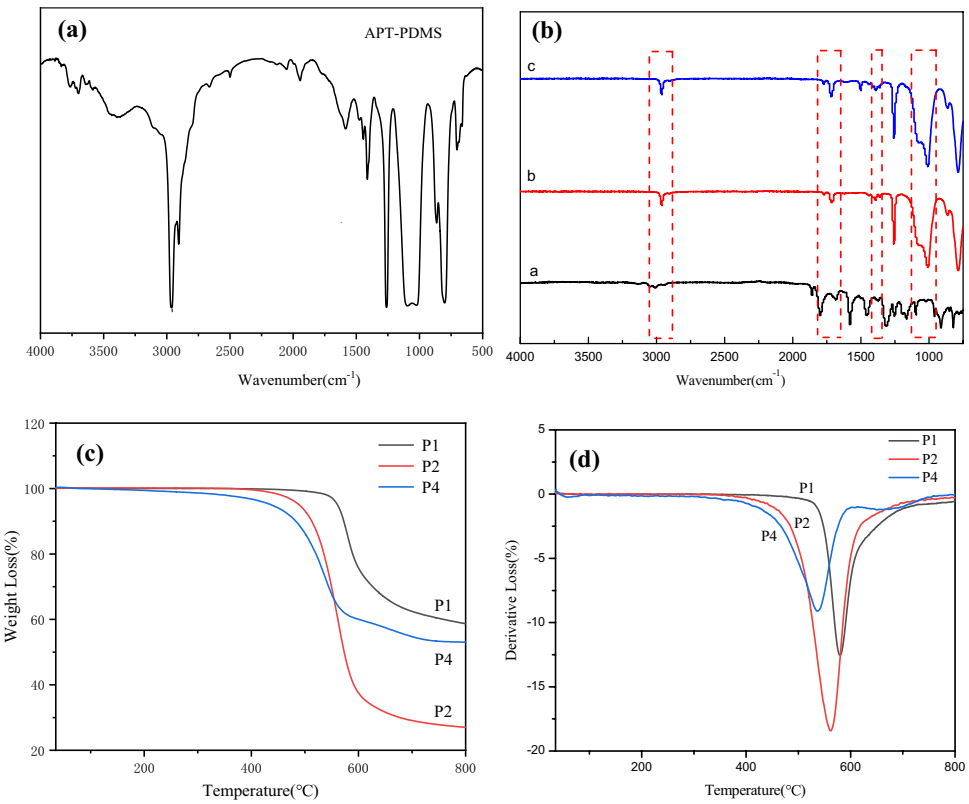

Fig. 2 (**a**) FTIR spectra of the APT-PDMS (**b**) FTIR spectra of the polyimides (a.P1 b.P2 c.P4) (**c**) TGA curves of the PI series under N_2 atmosphere (**d**) DTG curves of the PI series under N_2 atmosphere

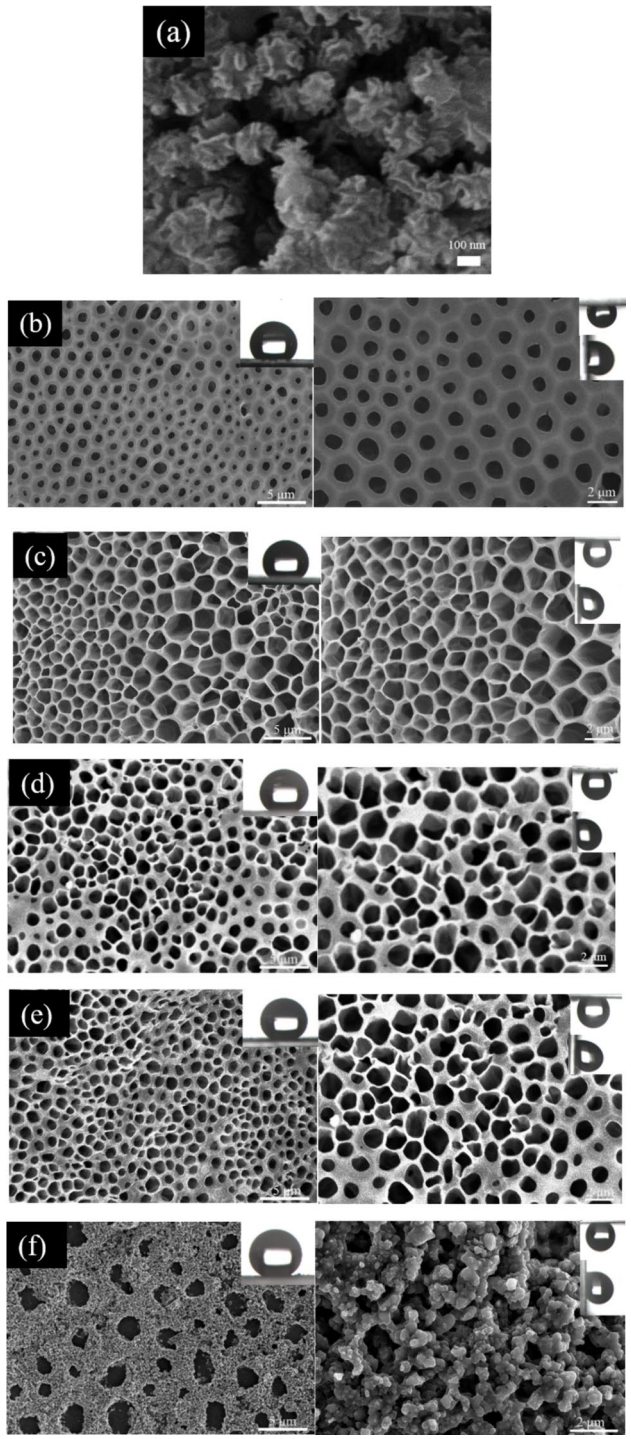

Fig. 3 SEM images of (**a**) KCC-1 and the porous films obtained for polymers (**b**) P1, (**c**) P2, (**d**) P3, (**e**) P4, (**f**) P5, (**g**) P6

As shown in Fig. 3, through BF, the substrate surface prepared by the P1-P6 polymer has formed holes. When the water drops to the porous surface, the air in the hole will lift the water drops to make them round, and the surface of P1-P6 porous substrate presents Wenzel state. The water drops are pinned on the surface, and will not fall off after turning 90° and 180°. P2 introduces a flexible segment (APT-PDMS) to form a siloxane-containing polyamide acid. During the self-assembly process, the molecular chain is easier to move, the formed holes are denser than P1, and the static contact angle is increased from 110° to 138°. Compared with Fig. 3(c), Fig. 3(d) formed a smaller hole size, because the introduction of KCC-1-NH2 transforms the linear polyimide chain into a crosslinked network structure, which restricts the molecular chain movement. At the same time, the introduction of inorganic nanometers increases the roughness, and the contact angle is further improved, reaching 142°. The ratio of KCC-1-NH_2 in Fig. 3(e) is 10%, the formed pores are about 1–2 μm, and the contact angle reaches 145°. As the ratio of KCC-1-NH_2 increases, the movement of molecular chains during self-assembly becomes more and more difficult. As shown in Fig. 3(f), the substrate surface is composed of large pores about 3 μm and countless small pores. The connection with the large hole is formed by the accumulation of numerous small holes, and the contact angle is 152°, which is super-hydrophobic. While (g) does not form obvious holes, its surface owns a certain roughness, and the contact angle is 151°.

Wettability analysis

From Tables 3 and 4, it can be seen that a series of polyimide SLIPS prepared with $CHCl_3$ as solvent have ultra-slippery properties. Water droplets can slide on the surface, which proves that the silicone oil is poured into the porous rough structure to form a continuous and uniform oil layer on the surface, and the sliding angle of SLIPS-P4 is the lowest, SA = 2°, as shown in Fig. 4. In Table 5, the sliding angles of SLIPS prepared by blending polyamide acid and mesoporous silica are higher than those of SLIPS prepared by polyimide compounded with silica.

Stability analysis

The stability of lubricating oil is the basis for the excellent performance of SLIPS. Under the time of long -term placement, the loss of lubricating oil will cause the exposure of the rough structure of hydrophobic oil, making the droplets and pollutants easily adhere to the surface. Therefore, good oil storage and oil locking ability are important features for the lubricating oil injection surface to maintain the interface performance for a long time. The durability of polyimide SLIPS was characterized by accelerated lubricating oil loss tests in harsh environments with high-temperature evaporation and high centrifugal shear.

The 6 groups of SLIPS were placed in an oven at 100 °C, and their contact angles, sliding angles and weights were recorded. At high temperature, the continuous and uniform

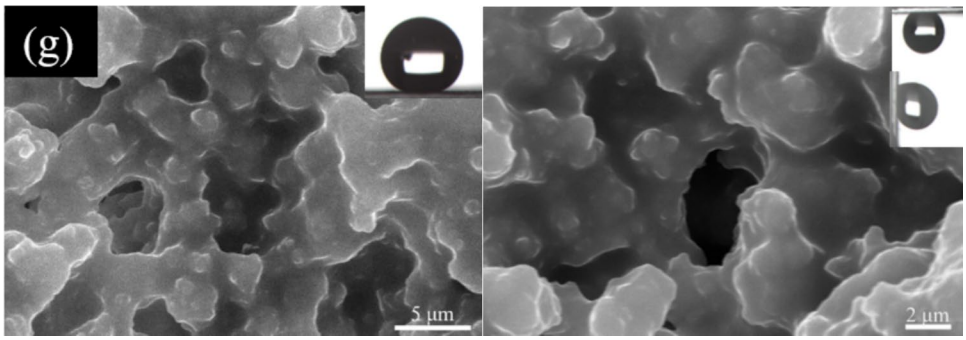

Fig. 3 (continued)

Table 3 Wettability analysis of porous membranes and SLIPS

	$CHCl_3$	The WCA of porous films	The CA of SLIPS	The SA of SLIPS	KCC-1-NH_2 ratio	KCC-1-NH_2:APT-PDMS
P1	30 mg/ml	110°	100°	10°	0	
P2		138°	103°	4°	0	
P3		142°	105°	3°	5%	1:12
P4		145°	104°	2°	10%	1:2.5
P5		152°	107°	3°	25%	1.5:1
P6		151°	110°	6°	40%	1.6:1

Table 4 Compare the SA of different SLIPS

Preparation Materials	Preparation method	SA	Reference
PTFE/$Zn(Ac)_2$/NaCl	dip-coating method	8.5°	[22]
PES/PVDF-HFP/APT-TiO_2	Sol–gel method/ Spraying method	10°	[23]
Glucose/PDMS	Template method	20°	[24]
APT-PDMS/KCC-1-NH_2/ BAPP/ S-BPDA	BF	2°	This work

Table 5 Wettability analysis of porous membranes and SLIPS prepared by blending PI and KCC-1

	$CHCl_3$	The WCA of porous films	The CA of SLIPS	The SA of SLIPS	KCC-1-NH_2 ratio
1	30 mg/ml	129°	100°	5°	5%
2		133°	101°	5°	10%
3		142°	104°	5°	25%
4		144°	106°	7°	40%

lubricating oil layer formed on the porous surface will be destroyed, exposing part of its rough structures and increasing the contact angle, as shown in Fig. 5(a). Among them, the contact angle of SLIPS-P4 increased from 104° to 108°, and the change was only 4°.

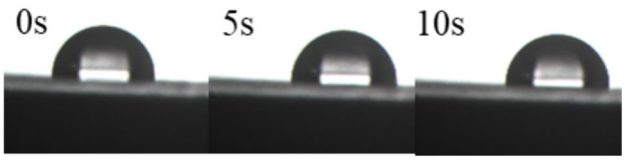

Fig. 4 Droplet sliding images on the SLIPS (P4)

Figure 5(b) shows the quality change of lubricating oil within 7 days, the evaporation rates of SLIPS-P1-P6 are 2.2%, 1.1%, 0.6%, 0.5%, 0.7%, 1.3% respectively, and the evaporation rate of SLIPS-P4 after 7 days is only 0.5%. Figure 6(d) shows the wetting property of the SLIPS over a 7 day period. The tilting angle was measured by examining a 5 μL water droplet slipping down the surfaces. The SLIPS-P4 is still the best.We speculate for three reasons: (1) Lubricating oil and network structure depend on the force between molecularity. Polyxia oil is similar to the silicane structure in polyanide, increasing the interaction. (2) Mesoporous silica itself can store part of the silicone oil. (3) SLIPS-P4 forms a closed-cell structure and has a large capillary force.

In the practical application of SLIPS, the larger shear force will destroy the capillary effect and reduce the oil holding capacity. To further characterize the lubricating stability of SLIPS, a glass flake sample was placed in the center of a spin coater, and the centrifugal force of the spin coater was used to simulate shear conditions. As shown in

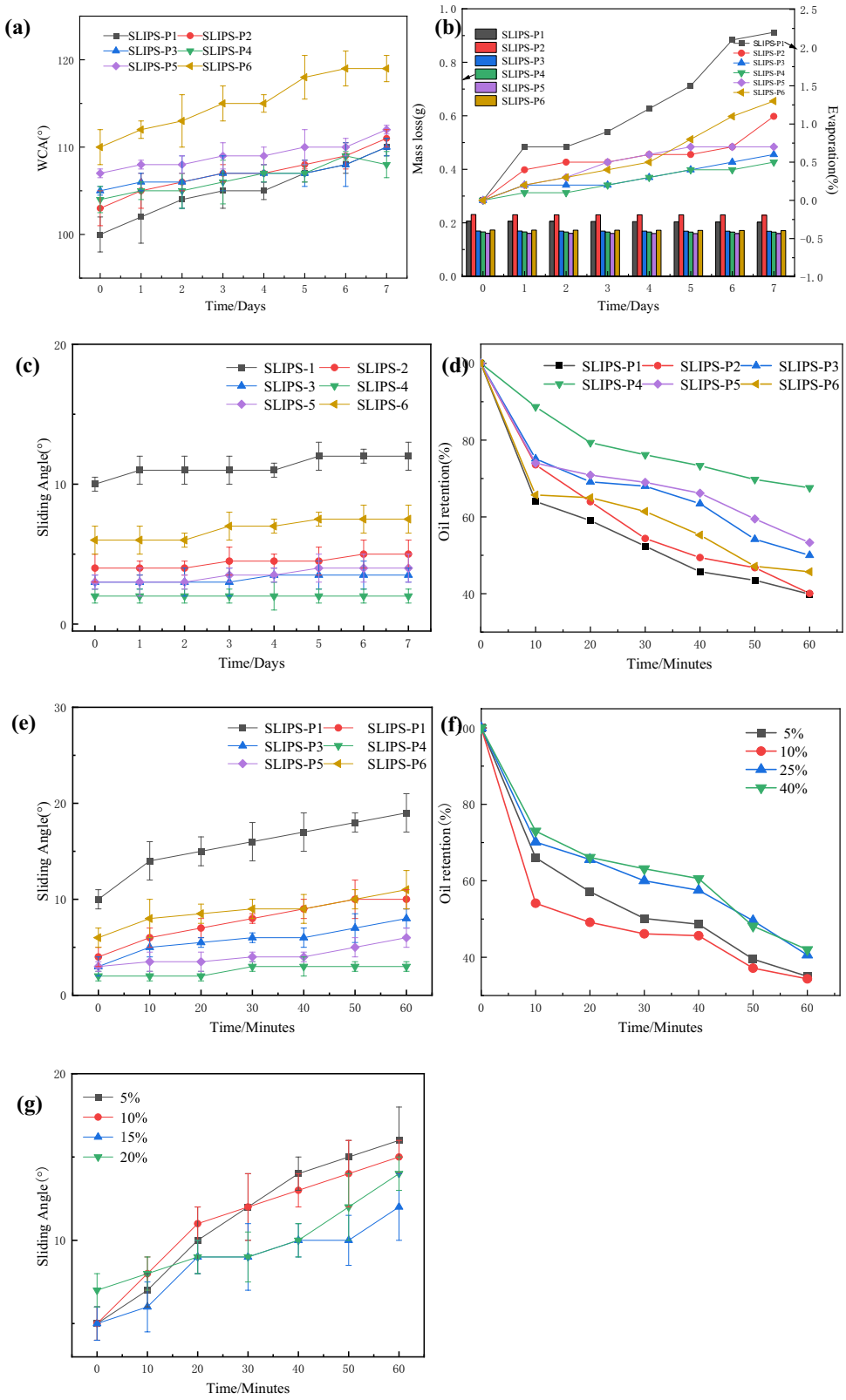

Fig. 5 (**a**) Variation of SLIPS static contact angle within 7 days; (**b**) Mass loss of the lubricant in the SLIPS over a 7 day period; (**c**) Wetting property of the SLIPS over a 7 day period; (**d**) Changes in oil locking rate of different polyimide SLIPS centrifugation for 60 min; (**e**) Changes in the sliding angle of different polyimide SLIPS centrifugation for 60 min; (**f**) Changes in oil locking rate of SLIPS prepared by blending PI and KCC-1 by centrifugation for 60 min; (**g**) Change of slip angle of SLIPS centrifugation prepared by mixing PI and KCC-1 for 60 min

Fig. 5(d), after rotating at 3000 rpm for 60 min, the oil locking rate of SLIPS-P1 is only 39.87%, while the remaining 5 groups were all higher than that of SLIPS-P1, because silicon oil is similar to the structure of P2-P6 molecular structure, it has higher affinity for porous rough structures and meets the principles of similar compatibility. In

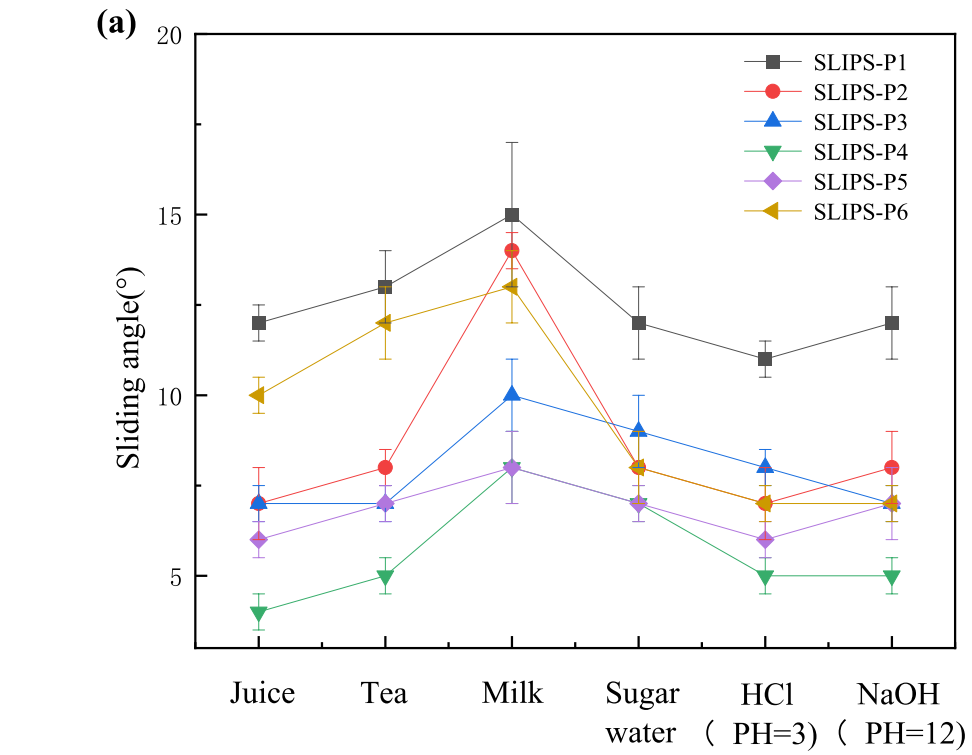

Fig. 6 (**a**) The sliding angle of different liquids on SLIPS surface (**b**) Wetting behavior of milk, sugar water, and juice on the SLIPS surface. (P4)

addition, the oil locking rate of SLIPS-P3-P6 is higher than that of SLIPS-P2, because the introduction of mesoporous silica can better lock oil. Compared with SLIPS of through-hole structure [25, 26], the pores formed by SLIPS-P4 are small in size and densely distributed, and the honeycomb-like pores are isolated from the adjacent pores by the film-like surface to form a single independent micro-structure, the lubricating oil is separated by a single microstructure, which can generate a large capillary force, block the loss of silicone oil, and improve the stability of the lubricating oil layer on the rough surface, and the oil locking rate is 67.58%. While the content of SLIPS-P5 silica is higher, the nanoparticles in the cross-linked network tend to be closer to the pore wall during the self-assembly process, which destroys the pore wall structure of the original honeycomb, and the formed porous structure is interconnected. When subjected to high shear force, the lubricating oil stored in the open-pore structure is easily lost, and the oil-locking rate is 53.3%. The sliding angle test was performed on SLIPSs treated under high shear conditions, as shown in Fig. 5(e). After simulating high shear conditions, the sliding angle of SLIPS-P1 increased from 10° to 19°, while the sliding angle of SLIPS-P4 only changed from 2° to 3°. The oil locking rates of four groups of SLIPS prepared by blending polyamide acid and mesoporous silica after centrifugation at 3000 rpm for 60 min were 35%, 34.34%, 37.73%,

40.58%, and 42% respectively, as shown in Fig. 5(f). The sliding angles of the four groups of SLIPSs under the condition of simulating high shear force were 11°, 10°, 7°, and 7°, respectively. The polyimide SLIPS prepared by blending has poor stability.

Antifouling analysis

Considering the complexity of the real environment, SLIPS needs to have good anti-fouling ability to effectively prevent various liquid pollutants. Therefore, the sliding angles of different liquids on different SLIPS were measured. As shown in Fig. 6(a), the sliding angles of common aqueous liquids on the SLIPS-P1-P6 surfaces were all lower than 20°. Among them, the sliding angles of various liquids on the surface of SLIPS-P3, SLIPS-P4, and SLIPS-P5 are all lower than 10°, and the antifouling ability is good. In order to further verify the antifouling ability of SLIPS-P4, milk, sugar water and fruit, juice were dropped on the surface of the sample piece with an inclination of 8°, after some time, the liquid slides to the bottom without any residue, as shown in Fig. 6(b).

Conclusion

In this paper, mesoporous silica was introduced into the main chain of polyamide acid, combined with the BF, the porous substrate of polyamide acid was prepared. The effect of APT-PDMS and the ratio of KCC-1-NH_2 on the performance of polyimide SLIPS was investigated. The results show that APT-PDMS not only increases the polymer amphiphilicity, which is conducive to the formation of uniform pores during the self-assembly of the polymer, but also improves the interaction between the lubricating oil and the substrate; At the same time, the introduction of mesoporous silica is conducive to the formation of a uniform and dense closed-cell structure, which improves the ability to store and lock oil. Among them, the polyimide SLIPS prepared with KCC-1-NH_2 ratio of 10% (SLIPS-P4) has the best comprehensive performance. The SLIPS-P4 has a sliding angle of 2° and has excellent self-cleaning and antifouling properties. It is placed in an environment of 100 °C for 7 days, the contact angle changes to 4°, the evaporation rate is only 0.5%, and under high shear conditions for 60 min, the oil locking rate of nearly 67.58% can be maintained, The change of the sliding angle is only 1 °. SLIPS-P4 has a good oil locking ability and has a certain potential to improve the service life of SLIPS. This paper provides a facile method to prepare low-cost, environmentally friendly and stable polyimide SLIPS, which is expected to be applied in the fields of self-cleaning and antifouling.

Acknowledgements The research is especially grateful for the sponsored by Support Program (Industrial) of Changzhou Science and Technology (CE 20220004), the Top-notch Academic Programs Project of Jiangsu Higher Education Institutions (TAPP) and the Jiangsu Province Higher Education Priority Academic Program Development Project (PAPD). The authors thank the Department of Mechanical Engineering, School of Petrochemical Engineering for providing laboratory facilities and instrumentation support.

Declarations

Conflict of interest No potential conflict of interest was reported by the author(s).

References

1. Guo XD, Dai Y, Gong M, Qu YG, Helseth LE (2015) Changes in wetting and contact charge transfer by femtosecond laser-ablation of polyimide. Appl Surf Sci 349:952–956
2. Zheng QF, Fang L, Guo HQ, Yang KF, Cai ZY, Meador MA, Gong SQ (2018) Highly porous polymer aerogel film-based triboelectric nanogenerators. Adv Funct Mater 28:1706365
3. He QF, Sun K, Wang ZX, Wang ZY, Yang PT, Tian JH, Duan WX, Fan RH (2022) Epsilon-negative behavior and its capacitance enhancement effect on trilayer-structured polyimide–silica/multiwalled carbon nanotubes/polyimide–polyimide composites. J Mater Chem C 11:4286–4294
4. Wu TT, Dong J, Gan F, Fang Y, Zhao TX, Zhang QH (2018) Low dielectric constant and moisture-resistant polyimide aerogels containing trifluoromethyl pendent groups. Appl Surf Sci 440:595–605
5. Min K, Kim Y, Goyal S, Lee SH, Mckenzie M, Park H, Savory ES, Rammohan AR (2016) Interfacial adhesion behavior of polyimides on silica glass: a molecular dynamics study. Polymer 98:1–10
6. Zhang D, Wang C, Wang QH, Wang TM (2019) High thermal stability and wear resistance of porous thermosetting heterocyclic polyimide impregnated with silicone oil. Tribol Int 140:105728
7. Martínez-Gómez A, Alvarez C, Abajo JD, Campo AD, Cortajarena A, Rodriguez-Hernandez J (2015) Poly (ethylene oxide) functionalized polyimide-based microporous films to prevent bacterial adhesion. ACS Appl Mater Inter 7:9716–9724
8. Breunig M, Dorner M, Senker J (2021) Ultramicroporous polyimides with hierarchical morphology for carbon dioxide separation. J Mater Chem A 9:12797–12806
9. Ye JZ, Li JB, Tao Q, Huang HB, Zhou NN (2021) Effects of surface pore size on the tribological properties of oil-impregnated porous polyimide material. Wear 484:204042
10. Tan LX, Tan B (2017) Hypercrosslinked porous polymer materials: design, synthesis, and applications. Chem Soc Rev 46:3322–3356
11. Zheng QF, Fang LM, Guo HQ, Yang KF, Cai ZY, Meador MA, Gong SQ (2018) Highly porous polymer aerogel film-based triboelectric nanogenerators. Adv Funct Mater 28:1706365
12. Zhang D, Tao LM, Wang QH, Wang TM (2016) A facile synthesis of cost-effective triphe-nylamine-containing porous organic polymers using different crosslinkers. Polymer 82:114–120
13. Wong TS, Kang SH, Tang S, Smythe EJ, Hatton BD, Grinthal A, Aizenberg J (2011) Bioinspired self-repairing slippery surfaces with pressure-stable omniphobicity. Nature 477:443–447
14. Qing YQ, Long C, An K, Liu CS (2022) Natural rosin-grafted nanoparticles for extremely-robust and eco-friendly antifouling coating with controllable liquid transport. Compos Part B-Eng 236:109797
15. Qi J, Chen Y, Zhang WT, Lei L, Huang HD, Lin H, Zhong GJ, Li ZM (2022) Imparting cellulose acetate films with hydrophobicity,

high transparency, and self-cleaning function by constructing a slippery liquid-infused porous surface. Ind Eng Chem Res 61:7962–7970
16. Stamatopoulos C, Hemrle J, Wang DH, Poulikakos D (2017) Exceptional anti-icing performance of self-impregnating slippery surfaces. ACS Appl Mater Inter 9:10233–10242
17. Liu C, Li YL, Lu CG, Liu Y, Feng S, Liu YH (2020) Robust slippery liquid-infused porous network surfaces for enhanced anti-icing/deicing performance. ACS Appl Mater Inter 12:25471–25477
18. Liu YB, Tian Y, Chen J, Gu HM, Liu J, Wang RM, Zhang BL, Zhang HP (2019) Design and preparation of bioinspired slippery liquid-infused porous surfaces with anti-icing performance via delayed phase inversion process. Colloid Surf A 588:124384
19. Tong ZM, Rao QQ, Chen S, Song LN, Hu JK, Hou Y, Gao X, Lu JG, Zhan XL, Zhang QH (2022) Sea slug inspired smart marine antifouling coating with reversible chemical bonds: controllable UV-responsive coumarin releasing and efficient UV-healing properties. Chem Eng J 429:132471
20. Tong ZM, Guo HG, Di ZG, Sheng Y, Song LN, Hu JK, Gao X, Hou Y, Zhan XL, Zhang QG (2022) Squid inspired elastomer marine coating with efficient antifouling strategies: hydrophilized defensive surface and lower modulus. Colloid Surf B 213:112392
21. Rao QQ, Tong ZM, Song LN, Ali A, Hou Y, He QG, Lu JG, Gao X, Zhan XL, Zhang QH (2021) NIR-driven fast construction of patterned-wettability on slippery lubricant infused surface for droplet manipulation. Chem Eng J 428:131141
22. Zhu Y, He Y, Yang DQ, Sacher E (2018) A facile method to prepare mechanically durable super slippery polytetrafluoroethylene coatings. Colloid Surf A 556:99–105
23. Yuan SC, Peng JW, Zhang XG, Lin D, Geng HL, Han B, Zhang M, Wang HY (2021) A mechanically robust slippery surface with 'corn-like' structures fabricated by in-situ growth of TiO_2 on attapulgite. Chem Eng J 415:128953
24. Qian HC, Liu B, Wu DQ, Liu WL (2021) Facile fabrication of slippery lubricant-infused porous surface with pressure responsive property for anti-icing application. Colloid Surf A 618:126457
25. TAS M, Memon H, Xu F, Ahmed I, Hou XH (2020) Electrospun Nanofibre membrane based transparent slippery liquid-infused porous surfaces with icephobic properties. Colloid Surf A 585:124177
26. Fan HF, Guo ZG (2021) WO_3-based slippery coatings with long-term stability for efficient fog harvesting. J Colloid Interf Sci 591:418–428